

Ginzburg-Landau theory for the conical cycloid state in multiferroics: applications to CoCr_2O_4

Chuanwei Zhang^{1,2}, Sumanta Tewari^{1,3}, John Toner⁴, and S. Das Sarma¹

¹Condensed Matter Theory Center, Department of Physics, University of Maryland, College Park, MD 20742

²Department of Physics and Astronomy, Washington State University, Pullman, WA 99164

³Department of Physics and Astronomy, Clemson University, Clemson, SC 29634

⁴Department of Physics and Institute of Theoretical Science, University of Oregon, Eugene, OR 97403

We show that the cycloidal magnetic order of a multiferroic can arise in the absence of spin and lattice anisotropies, for e.g., in a cubic material, and this explains the occurrence of such a state in CoCr_2O_4 . We discuss the case when this order coexists with ferromagnetism in a so called ‘conical cycloid’ state, and show that a direct transition to this state from the ferromagnet is necessarily first order. On quite general grounds, the reversal of the direction of the *uniform* magnetization in this state can lead to the reversal of the electric polarization as well, without the need to invoke ‘toroidal moment’ as the order parameter.

PACS numbers: 75.80.+q, 77.80.Fm, 75.30.Fv, 75.10.-b

I. INTRODUCTION

Ferromagnetism and ferroelectricity are two of the most well-known and technologically relevant types of long range ordering that can occur in solids. It is therefore of paramount interest and importance that in a class of ternary oxides, known as “multiferroics”, both types of order seem to co-exist with the possibility of interplay between long range magnetism and long range electric polarization^{1,2,3,4}. The recently discovered new class of multiferroics with strong magnetoelectric effects often display the coexistence of a spatially modulated magnetic order, called ‘cycloidal’ order, and uniform polarization (\mathbf{P}), which is induced by the broken inversion symmetry due to the modulation of the magnetization^{5,6}. Since \mathbf{P} is inherently of magnetic origin, unusual magnetoelectric effects, as displayed by the ability to tune the polarization by a magnetic field which acts on the cycloidal order parameter, are possible, opening up many applications^{2,7,8,9,10,11,12,13,14,15}. Among this exciting class of materials, the cubic spinel oxide CoCr_2O_4 is even more unusual, since it displays not only a non-zero \mathbf{P} and a spatially *modulated* magnetic order, but also a *uniform* magnetization¹⁵ (\mathbf{M}) in a so-called ‘conical cycloid’ state (see below). The uniform component of \mathbf{M} provides an extra handle² with which to tune \mathbf{P} , as has been recently demonstrated¹⁵. The low value of the required tuning magnetic field $\sim .5$ T, makes this material even more experimentally appealing.

The ability to tune \mathbf{P} by tuning the uniform part of \mathbf{M} poses a theoretical puzzle, since, in existing theories, the uniform piece of \mathbf{M} should not influence the polarization at all^{5,6,16,17}. This has led to the introduction of the ‘toroidal moment’, $\mathbf{T} = \mathbf{P} \times \mathbf{M}$, as the real order parameter characterizing the conical cycloid state of CoCr_2O_4 ¹⁵. In this Letter, we explain this unique phenomenon and the other interesting aspects of the physics of the conical cycloid state by developing a phenomenological Ginzburg-Landau (GL) theory. Additionally, the rotationally invariant form of the theory proves that both the ordinary and the conical cycloidal orders, with the resulting multiferroicity, are possible even in systems *without* easy plane spin and easy axis lattice anisotropies. This is important since earlier models^{2,5,18} of the cycloidal state depend cru-

cially on such anisotropies. However, such anisotropic models can *not* explain the presence of the cycloidal state in cubic systems like CoCr_2O_4 , where such phases are also observed despite the fact that their cubic symmetry forbids such easy plane and easy axis anisotropies.

CoCr_2O_4 , with the lattice structure of a cubic spinel, enters into a state with a uniform magnetization at a temperature $T_m = 93$ K. Microscopically, the magnetization is of ferrimagnetic origin¹⁵, and in what follows we will only consider the ferromagnetic component, \mathbf{M} , of the magnetization of a ferrimagnet. At a lower critical temperature, $T_c = 26$ K, the system develops a special helical modulation of the magnetization in a plane transverse to the large uniform component. Such a state can be described by an order parameter,

$$\mathbf{M}_h = m_1 \hat{e}_1 \cos(\mathbf{q} \cdot \mathbf{r}) + m_2 \hat{e}_2 \sin(\mathbf{q} \cdot \mathbf{r}) + m_3 \hat{e}_3 + h.h., \quad (1)$$

where $\{\hat{e}_i\}$ form an orthonormal triad and *h.h.* denotes “higher harmonics” such as terms proportional to sines and cosines of $(2n+1)\mathbf{q} \cdot \mathbf{r}$ with integer n . When the pitch vector, \mathbf{q} , is normal to the plane of the rotating components, the rotating components form a conventional helix¹⁹. For $m_3 = 0$ such a state, which we call an ‘ordinary helix’ state, is observed in many rare-earth metals²⁰, e.g. MnSi ^{21,22}, and FeGe ²³. We call a helix state with $m_3 \neq 0$, which is observed in some heavy rare-earth metals²⁰, a ‘conical helix’ state because the tip of the magnetization falls on the edge of a cone. A more complicated modulation arises when \mathbf{q} lies *in the plane* of the rotating components. For $m_3 = 0$, we call such a state an ‘ordinary cycloid’ state because the profile of the magnetization resembles the shape of a cycloid. The state with $m_3 \neq 0$ is called a ‘conical cycloid’ state. It is easy to see that the helical, but not the cycloidal, modulation preserves a residual symmetry under translations and suitable simultaneous rotations about the pitch vector.

Since \mathbf{M} and \mathbf{P} respectively break time reversal and spatial inversion symmetry, the leading \mathbf{P} -dependent piece in a GL Hamiltonian density, h_P , for a centrosymmetric, time reversal invariant system with cubic symmetry is⁵,

$$h_P = \mathbf{P}^2/2\chi + \alpha \mathbf{P} \cdot \mathbf{M} \times \nabla \times \mathbf{M}, \quad (2)$$

where $\chi > 0$ and α are coupling constants. We assume that \mathbf{P} is a slave of \mathbf{M} , in the sense that a non-zero \mathbf{P} only oc-

curs due to the spontaneous development of a magnetic state with a non-zero $\mathbf{M} \times \nabla \times \mathbf{M}$, which then, through the linear coupling to \mathbf{P} in (2), induces a non-zero \mathbf{P} . For an order parameter ansatz given by Eq. 1, the macroscopic polarization, $\bar{\mathbf{P}}$, is given by minimizing the Hamiltonian density (2) over \mathbf{P} , $\bar{\mathbf{P}} = \chi\alpha m_1 m_2 [\hat{e}_3 \times \mathbf{q}]$. So $\bar{\mathbf{P}}$ is normal to both \mathbf{q} and the axis of rotation, \hat{e}_3 . Note that in a conventional spin density wave state (m_1 or $m_2 = 0$), as in the helix states, $\bar{\mathbf{P}}$ is zero. However, for a cycloid state, $\mathbf{q} \perp \hat{e}_3$, so there is a non-zero $\bar{\mathbf{P}}$. Note that $\bar{\mathbf{P}}$ is entirely due to the cycloidal components m_1 and m_2 , and is independent of the uniform magnetization m_3 . Thus, while it is conceivable that magnetic fields strong enough to ‘flop’ the spins and the axis of rotation of the cycloidal components will alter $\bar{\mathbf{P}}$ ^{5,6,7,8}, no explanation of how tuning the uniform component of \mathbf{M} can affect the induced polarization has been offered. We will do so later in this paper.

The paper is organized as follows: Section II lays out the Ginzburg-Landau Hamiltonian and the parameter regions which exhibits the cycloidal phase. Section III and V are devoted to the phase diagrams of ordinary cycloidal state and conical cycloidal state respectively. In Section V, we explain why the reversal of the direction of the uniform magnetization in the conical cycloidal state can lead to the reversal of electric polarization. Section VI consists of conclusions.

II. GINZBURG-LANDAU HAMILTONIAN

We consider a Hamiltonian that is *completely* invariant under simultaneous rotations of positions and magnetization. This guarantees that any phase that can occur in our model is *necessarily* allowed in a crystal of *any* symmetry. The full Hamiltonian is given by, $H = \int (h_M + h_P) d\mathbf{r} \equiv \int h d\mathbf{r}$. Using $\mathbf{P} = -\chi\alpha \mathbf{M} \times \nabla \times \mathbf{M}$ to eliminate \mathbf{P} , we can write the total Hamiltonian density h entirely in terms of \mathbf{M} ,

$$\begin{aligned} h = & t\mathbf{M}^2 + u\mathbf{M}^4 + K_0(\nabla \cdot \mathbf{M})^2 + K_1(\nabla \times \mathbf{M})^2 \\ & + K_2\mathbf{M}^2(\nabla \cdot \mathbf{M})^2 + K_3(\mathbf{M} \cdot \nabla \times \mathbf{M})^2 \\ & + K_4|\mathbf{M} \times \nabla \times \mathbf{M}|^2 \\ & + D_L|\nabla(\nabla \cdot \mathbf{M})|^2 + D_T|\nabla(\nabla \times \mathbf{M})|^2, \end{aligned} \quad (3)$$

where we have $u, D_{L,T} > 0$ for stability. In Eq. 3, where the Landau expansion of the free energy is truncated at the fourth order, the usual gradient-squared term, $c|\nabla\mathbf{M}|^2$, is omitted since, $|\nabla\mathbf{M}|^2 = (\nabla \cdot \mathbf{M})^2 + |\nabla \times \mathbf{M}|^2$, plus an unimportant surface term which can be neglected. Notice that, for $K_0 = K_1$ and $K_2 = K_3 = K_4$, h is rotationally invariant in the spin space alone, so the K_i ’s themselves are not proportional to the spin-orbit coupling constant (for e.g., via the above identity, $K_0, K_1 \sim c$). However, the *difference* among the K_i ’s should be small due to the smallness of the spin-orbit coupling. The effects of the competing magnetic interactions, which are present in the multiferroics and are responsible for the spatial modulation of \mathbf{M} ^{2,5,17,18}, are embodied in K_0, K_1 , which can be negative leading to a spatially modulated order parameter. For decoupled spin and coordinate spaces (K_i ’s

equal), the energies of the helical and the cycloidal modulations of the spins are identical. In a system where the spin anisotropy constrains the spins to lie on a plane, and the lattice anisotropy forces \mathbf{q} to be also on that plane, the energy of the cycloidal modulation can be lower than that of the helical modulation^{5,18}. Such anisotropies have been implicitly taken as the driving force behind the cycloidal order by Mostovoy⁵, and Katsura *et al.*¹⁸. For cubic crystals, however, no such anisotropy exists among the principal directions. We argue below that, in this case, the magnetoelectric couplings themselves, leading to the difference among the K_i ’s, can lower the energy of the cycloidal state than that of any other state with an arbitrary angle between \mathbf{q} and the plane of the magnetization.

Rather than exploring the complete parameter space of this model, we limit ourselves to two different parameter regions, which exhibit all the phases described above:

Region I: $K_{0,1} < 0, K_{i>1}$ small, $t > 0$, and

Region II: $t < 0, K_3 < 0, K_1 > 0, K_2 = K_4 = 0$.

We have checked that our results are robust against allowing small non-zero values of the various K_i ’s that we take to be zero. In that sense our results, in particular the topology of the phase diagrams shown in Figs. 1a and 2a for Regions I and II, respectively, and the orders of the various phase transitions that we predict, are generic. As usual, our theoretical phase diagrams can be related to experimental ones by noting that *all* of the phenomenological parameters ($t, K_i, D_{L,T}, u$) in our model should depend on experimental parameters like, e.g., temperature (T). Thus, an experiment in which, e.g., T is varied with all other parameters held fixed will map out a locus of points through our theoretical phase diagrams. In Landau theories, t is expected to vary from large positive values, corresponding to disordered phases with $\mathbf{M}(\mathbf{r}) = \mathbf{0}$, at high T , to smaller values at which $\mathbf{M}(\mathbf{r}) \neq \mathbf{0}$ become possible. In order to access the conical cycloid state, we must also allow $K_0(T)$ and $K_1(T)$ to change sign as T is decreased.

For the most part we will work in mean field theory, which is simply finding a magnetization configuration $\mathbf{M}(\mathbf{r})$ that minimizes the Hamiltonian (3). Clearly, the task of finding the *global* minimum is a formidable one. Instead, we restrict ourselves to ansatzes of the form:

$$\mathbf{M} = m_1 \hat{e}_1 \cos(\mathbf{q} \cdot \mathbf{r}) + m_2 \hat{e}_2 \sin(\mathbf{q} \cdot \mathbf{r}) + \mathbf{M}_0, \quad (4)$$

where the spatially constant vector \mathbf{M}_0 is allowed to point in *any* direction. (Given the global rotation invariance under simultaneous rotations of magnetization and space, an infinity of other solutions trivially related to (4) by such rotations, and with exactly the same energy, also exist, of course.) In the special case of \mathbf{q} along x direction (or, equivalently, anywhere in the $x - y$ -plane), this is a cycloid state with a uniform background magnetization $\mathbf{M}_0 = (M_{01}, M_{02}, M_{03})$. When \mathbf{q} is along z direction, it is a helix state. Inserting this ansatz (4) into the Hamiltonian (3), and integrating over the volume V of the system, we can obtain the energy of the system. Through the minimization of the energy, we find the conical cycloid state is the *only* state with a non-zero \mathbf{M}_0 when $K_3 < K_4$. In addition, the optimal direction for \mathbf{q} is *always* either in the ($x - y$) plane, or orthogonal to it. Putting these facts together

means that *all* of the minimum energy configurations are of the form (1). Furthermore, when \mathbf{q} lies in the $(x - y)$ plane, we can always use the global rotation invariance of our model to rotate \mathbf{q} to lie along the x -axis, and will henceforth do so.

III. ORDINARY CYCLOID STATE

In **Region I**, the dominant terms in the Hamiltonian involving the uniform component m_3 are $tm_3^2 + um_3^4$, therefore the lowest energy states have $m_3 = 0$. Small negative $K_{i>1}$ clearly cannot change this fact. The energy for the ordinary cycloid (OC) state is obtained by inserting (1) with $m_3 = 0$ into the Hamiltonian

$$E/V = \Gamma_L(q) m_1^2 + \Gamma_T(q) m_2^2 + u\Phi(m_1^2, m_2^2), \quad (5)$$

where $\Gamma_L(q) = (t + K_0q^2 + D_Lq^4)/2$, $\Gamma_T(q) = (t + K_1q^2 + D_Tq^4)/2$, and $\Phi(m_1^2, m_2^2) = 3(m_1^4 + m_2^4)/8 + m_1^2m_2^2/4$. In writing this, we have neglected the higher harmonics in Eq. (1), whose amplitude vanishes much faster (specifically, as fast or faster than $|m_i|^3$) than the magnitude of the order parameter itself, and thus have negligible effects on the phase boundaries. For large positive t , all the terms in this energy are positive, and, hence, the lowest energy state is $m_1 = m_2 = 0$; i.e., the paramagnet. As T decreases, t becomes smaller and the first phase transition that will occur depends on whether the minimum over q of $\Gamma_L(q)$ or $\Gamma_T(q)$ becomes negative first. For $r \equiv K_1/K_0 < \sqrt{D_L/D_T}$, $\Gamma_L(q)$ becomes negative first at $t_{OLS} = K_0^2/4D_L$, and m_1 starts to be nonzero. This boundary between paramagnet and the ordinary longitudinal spin density wave (OLS) phase ($m_2 = m_3 = 0, m_1 \neq 0$) is the horizontal (solid blue) line in the phase diagram Fig. 1a in the (r, t) plane for fixed negative K_0 and all $K_{i>1} = 0$.

The OLS phase will, as we continue lowering t , eventually become unstable to a non-zero m_2 ; this is the OC state. By minimizing the energy (5) in the OLS phase, we find $q^2 = q_{L,min}^2 = -K_0/2D_L$ and $m_1^2 = 2(t_{OLS} - t)/3u$. Inserting these into (5) we find that the coefficient of m_2^2 becomes negative below $t_{LOC} = t_{OLS}[3r - (1 + 3D_T/D_L)]/2$. This

value t_{LOC} of t therefore defines the locus of a continuous OLS-OC phase transition, and is the non-horizontal straight (solid (blue)) line in the $r - t$ plane shown in Fig. 1a.

For $r > \sqrt{D_L/D_T}$, Γ_T becomes non-zero first, which seems to imply that one enters the ordinary transverse spin density wave (OTS) phase ($m_1 = m_3 = 0, m_2 \neq 0$) first for large r . However, it is not true because the OTS phase always has higher energy than the ordinary helical (OH) phase. The energy for the ordinary helix state is

$$E/V = \Gamma_T(m_1^2 + m_2^2) + \Phi(m_1^2, m_2^2). \quad (6)$$

The minimization of the energy over the direction of (m_1, m_2) vector yields $|m_1| = |m_2| = m_H/\sqrt{2}$, that is, a *circular* helix. Further minimization over m_H and q gives the energy E_{OH} of the ordinary helix state $E_{OH}/V = -(t_{OH} - t)^2/4u$ for $t < t_{OH}$, where $t_{OH} = r^2 D_L t_{OLS}/D_T$. The energy for the OTS state is $E_{OTS}/V = -(t_{OH} - t)^2/6u$, which is obtained from equation (5) by setting $m_1 = 0$ and $q^2 = q_{T,min}^2 \equiv -\frac{K_1}{2D_T}$, and then minimizing over m_2 . E_{OTS} is clearly higher than E_{OH} . Hence, the helical state is always favored over the OTS state throughout Region I of the phase diagram. Note that t_{OH} defines the boundary for the second order transition from the paramagnet to the OH state.

There is also a direct first order phase transition between the OH and the OLS states along the line where $E_{OH} = E_{OLS}$. Here $E_{OLS}/V = -(t_{OLS} - t)^2/6u$ is the energy for OLS state obtained from equation (5). This equality yields the first order phase boundary $t_{OLH} = (\sqrt{3/2}t_{OH} - t_{OLS})/(\sqrt{3/2} - 1)$ between the OH and the OLS states (the dotted (green) line). The line for the OLS-OC transition always intersects the first order OLS-OH phase boundary before crossing the paramagnet-OLS boundary. This therefore always yields the topology shown in Fig. 1a.

A typical experimental locus through this phase diagram, namely one in which t decreases as temperature T does, with r constant, is shown in Fig. 1a. The sequence of phases that results is illustrated in Fig. 1b. We see that the paramagnet to ordinary cycloid phase transition is always preempted by a paramagnet to OLS phase transition, and the cycloid state is always elliptical. Both of these predictions are borne out by recent experiments on TbMnO_3 ^{13,14}. On the other hand, a direct transition to the circular helix state is predicted by our theory, and has indeed been observed experimentally^{21,22}.

All of the above statements are based on mean field theory, that is theory without considering the fluctuations. Going beyond mean field theory, very general arguments due to Brazovskii²⁴ imply that, in rotation invariant models, *any* direct transition from a homogeneous state (paramagnet) to a translationally ordered one (OLS and OH) *must* be driven first order by fluctuations. Consideration of topological defects and orientational order^{25,26,27} supports this conclusion, but raises the additional possibility that direct transition between the homogeneous and the translationally ordered phases could split into two, with an intermediate orientationally ordered phase, analogous to the 2D ‘‘hexatic’’ phase²⁸. In the present context, this implies that both the paramagnet to OLS and OH phase transitions are either driven first order by fluctuations, or

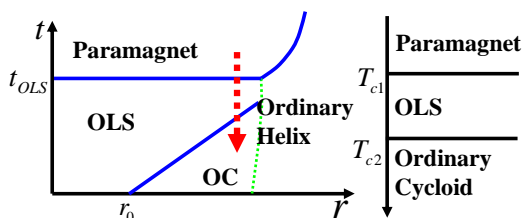


FIG. 1: (Color online) (a) Phase diagram in Region I for the ordinary cycloid state. Solid (blue) lines represent second order phase transitions. Dotted (green) line indicates the first order transition to the helix state. The dotted (red) arrow represents one possible schematic locus of the experimental points obtained by varying T . $r_0 \equiv (1 + 3D_T/D_L)/6$. (b) The sequence of phases with decreasing T along the locus shown.

split into two transitions with an intermediate orientationally ordered phase. Crystal symmetry breaking fields neglected in our model could invalidate this conclusion, if strong enough.

IV. CONICAL CYCLOID STATE

In **Region II**, we can show that conical cycloid (CC) state of the form $\mathbf{M} = (m_1 \cos(qx), m_2 \sin(qx), m_3)$ is the lowest energy state among all the possible states with arbitrary mutual angles between the uniform magnetization, \mathbf{q} , and the cycloid plane. The energy E for this state takes the form

$$\begin{aligned} E/V = & (t + K_0 q^2 + D_L q^4 + 2um_3^2) m_1^2/2 \quad (7) \\ & + (t + K_1 q^2 + D_T q^4 + 2um_3^2 + K_3 q^2 m_3^2) m_2^2/2 \\ & + u\Phi(m_1^2, m_2^2) + tm_3^2 + um_3^4, \end{aligned}$$

where we have again neglected the higher harmonics in Eq. (1). In this region, the *h.h.* terms do not vanish as the conical longitudinal spin density wave (CLS) ($m_2 = 0, m_{1,3} \neq 0$) or conical transverse spin density wave (CTS) ($m_1 = 0, m_{2,3} \neq 0$) to FM transition in Fig. 2 is approached. However, we have verified that amplitudes of the *h.h.* terms are only a very small fraction of the cycloidal components m_1 and m_2 (not of the uniform component m_3), therefore their neglect below (but close to) the lower cycloidal transition temperature of 26 K is justified. They have little or no quantitative effect on our phase diagram or the orders of the transition.

Since $t < 0$, we can minimize Eq. (7) over m_3 with $m_1 = m_2 = 0$, and find a ferromagnetic (FM) state with $m_3 = \sqrt{-t/2u}$. For large positive K_0 and K_1 , this ferromagnetic state is clearly stable against the development of non-zero m_1 and m_2 . It also clearly becomes *unstable* against the development of a non-zero m_1 if K_0 is lowered to negative values, because then the coefficient ($K_0 q^2 + D_L q^4$) of m_1^2 becomes negative for sufficiently small q . This instability (which is clearly into the CLS state) will occur at $K_0 = 0$, at a wavevector q satisfying $q_{L,min}^2 = -K_0/2D_L$. Note, however, that now, because K_0 is being varied *through* zero, this wavevector will now *vanish* as the transition is approached from below. The order parameter $m_1^2 = K_0^2/2uD_L$ also vanishes as this transition is approached. Thus, this transition is, like the β -incommensurate transition in quartz and berlinite²⁹, simultaneously a *nucleation* transition (q vanishes), and an *instability* transition (order parameter vanishes). Indeed, this transition and the FM \rightarrow CTS transition, which is of the same type and will be discussed below, are, to our knowledge, the *first* examples of transitions that exhibit such a dual character in a model *without* terms linear in the gradient operator.

We can find the loci of instability between the CLS phase and the CC state by calculating the coefficient of m_2^2 in (7) in the CLS phase, and finding where it becomes negative. The minimization of the energy (7) over q, m_3 and m_1 yields $q^2 = -K_0/2D_L$, $m_3^2 = -(t + K_0^2/2D_L)/2u$ and $m_1^2 = K_0^2/2uD_L$. Inserting these expressions into (7) and taking the coefficient of m_2^2 to be zero, we find the CLS to CC

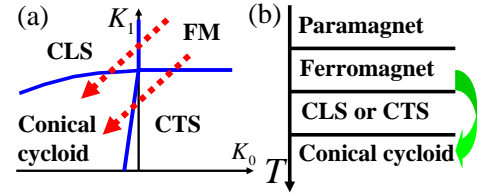


FIG. 2: (Color online) (a) Phase diagram in Region II for the conical cycloid state. Solid (blue) lines are the boundaries between different phases. The dotted (red) arrows represent possible paths for transition to the CC state via continuous transitions. (b) The succession of the phases with decreasing T . The (green) arrow represents a direct first order transition between the FM and the CC state.

phase boundary as:

$$K_1 = \frac{K_0}{2} \left(\frac{D_T}{D_L} - 1 + \frac{K_0 K_3}{2uD_L} \right) + \frac{tK_3}{2u}. \quad (8)$$

Similar analysis of the sequence of the phase transition, FM \rightarrow CTS \rightarrow CC, yields the schematic phase diagram on the $K_0 - K_1$ plane given in Fig. 2a. The phase boundary between FM and CTS is given by $K_1 = tK_3/2u$. The phase boundary between the CTS and the CC phase at small K_0 is $K_1 = 2K_0/(D_L/D_T - 1)$, which is also shown in Fig. 2a.

Fig. 2 shows that it is not possible to go from the FM to the CC state via a continuous transition, except at a single special point. Generic paths like the diagonal dashed lines in Fig. 2a *must* go through either the CLS or the CTS state, so two transitions are required to reach the CC state, which, additionally, must be elliptical. Hence the only way there can be a direct transition from the FM state to the CC state is via a first order phase transition, which is not addressed by our theory. This prediction is borne out by experiments of CoCr_2O_4 , where the direct FM to CC transition is indeed first order¹⁵.

V. MAGNETIC REVERSAL OF THE ELECTRIC POLARIZATION:

The polarization $\bar{\mathbf{P}} = \chi\alpha m_1 m_2 \hat{y}$ in the CC state is in the xy plane, normal to \hat{e}_3 and \mathbf{q} . It is independent of the uniform magnetization, m_3 . Experimentally¹⁵, the sample is cooled through T_c in the presence of a small electric field, $\mathbf{E} = E_0 \hat{y}$, and a small magnetic field, $\mathbf{H} = H_0 \hat{z}$. The direction of the pitch vector, \hat{x} , or, equivalently, the axis of rotation, \hat{z} , are set by the direction of $\bar{\mathbf{P}}$ (\mathbf{E}), which determines the ‘helicity’ of the cycloid⁷. It is found, at first, that $\bar{\mathbf{P}}$ is uniquely determined by \mathbf{E} alone, independent of the *initial* direction of \mathbf{H} , as expected. However, once $\bar{\mathbf{P}}$ and m_3 have set in, changing H_0 to $-H_0$ not only reverses the direction of m_3 , but also, quite unexpectedly, reverses the direction of $\bar{\mathbf{P}}$ as well. In the literature^{2,15}, this has led to the definition of the ‘toroidal moment’, $\mathbf{T} = \bar{\mathbf{P}} \times \mathbf{M}$, as the order parameter.

It is clear that the experimental system is in the conical cycloid state, where m_3, \mathbf{q} and $\bar{\mathbf{P}}$ are always in mutually orthogonal directions¹⁵. Further, as expected for this state, the directions of m_3 and $\bar{\mathbf{P}}$ are uniquely determined by the small

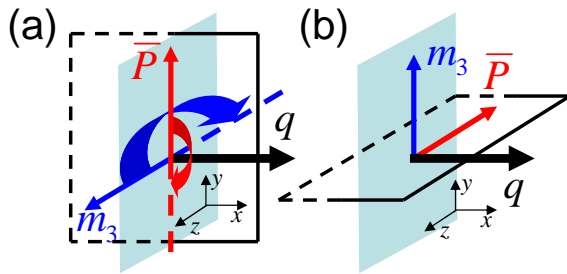


FIG. 3: The reversal of the polarization ($\bar{\mathbf{P}}$) by the reversal of the magnetization (m_3). (a) If m_3 rotates to $-m_3$, remaining perpendicular to \mathbf{q} , the cycloidal (xy) plane must rotate accordingly to always remain transverse to m_3 , which is the lowest energy configuration. Since $\bar{\mathbf{P}}$ is in the cycloidal plane, it will rotate by a total angle π . (b) An intermediate stage when m_3 has rotated by an angle $\frac{\pi}{2}$ and points in the \hat{y} direction. At this stage, $\bar{\mathbf{P}}$ points in the $-\hat{z}$ direction.

cooling fields, \mathbf{H} and \mathbf{E} , respectively, which add terms to the Hamiltonian that split the degeneracy between the minima corresponding to the different directions. Now assume that the direction of \mathbf{H} is reversed, $H_0 \rightarrow -H_0$, reversing the direction of m_3 once it has well developed. There are two ways the uniform magnetization can reverse its direction. First, m_3 may continue to remain along the z -axis and its magnitude may pass through zero to become $-m_3$ for $\mathbf{H} = -H_0\hat{z}$. If this is the case, $\bar{\mathbf{P}}$ will remain fixed in the direction \hat{y} , since the mutual orthogonality of m_3 , \mathbf{q} and $\bar{\mathbf{P}}$ can always be maintained and there is no direct coupling between m_3 and $\bar{\mathbf{P}}$. However, since m_3 is already well developed and large ($T_m = 93$ K), due to the magnetic exchange energy cost it may be energetically more favorable to leave the magnitude of m_3 unchanged, and its direction may rotate in space to $-\hat{z}$. If this is the case, then m_3 must rotate staying on the $y-z$ plane, since that way it always remains perpendicular to

\mathbf{q} , whose direction fluctuations cost the crystalline anisotropy energy. It is then clear, see Fig. 3, that the cycloid plane itself, which is always perpendicular to m_3 to maintain the lowest energy configuration, must rotate about \hat{x} by a total angle π . It follows that $\bar{\mathbf{P}}$, always on the cycloid plane, reverses its direction to $-\hat{y}$. This way, even though there is no dynamical coupling between m_3 and $\bar{\mathbf{P}}$, the latter can also rotate by an angle π as a result of the former reversing its direction in space. Based on this, we predict that, at some intermediate $\mathbf{H} \sim -H'\hat{z}$, where $H' < H_0$, $\bar{\mathbf{P}}$ points in the direction $-\hat{z}$, which can be experimentally tested.

VI. CONCLUSIONS

To conclude, we've shown that the magnetic cycloidal orders, and the resulting multiferroicity, can naturally arise due to the magnetoelectric couplings even in rotationally invariant systems, or in cubic crystals. This explains such orders in CoCr_2O_4 , which lack easy plane anisotropies, and are hence outside the realm of the previous theoretical studies on multiferroics. We also predict that a second order transition from the ferromagnet to the conical cycloid state can only occur through an intervening conical longitudinal or transverse spin density wave state with the ultimate cycloidal state being elliptical. A direct such transition, then, must be first order. An important feature of our Ginzburg-Landau theory is that we do not need to invoke an arbitrary (and ad hoc) 'toroidal moment' to explain the interplay between the magnetization and the polarization – the behavior which has been attributed to the toroidal moment arises naturally in our theory.

We thank D. Drew, D. Belitz, and R. Valdes Aguilar for useful discussions. This work is supported by NSF, NRI, LPS-NSA, and SWAN.

-
- ¹ M. Fiebig, J. Phys. D: Appl. Phys. **38**, R123 (2005).
² S.-W. Cheong and M. Mostovoy, Nature Materials **6**, 13 (2007).
³ Y. Tokura, Science **312**, 1481 (2006).
⁴ R. Ramesh and N.A. Spaldin, Nature Materials **6**, 21 (2007).
⁵ M. Mostovoy, Phys. Rev. Lett. **96**, 067601 (2006).
⁶ G. Lawes, A. B. Harris, T. Kimura, N. Rogado, R. J. Cava, A. Aharony, O. Entin-Wohlman, T. Yildirim, M. Kenzelmann, C. Broholm, and A. P. Ramirez, Phys. Rev. Lett. **95**, 087205 (2005).
⁷ T. Kimura, T. Goto, H. Shintani, K. Ishizaka, T. Arima and Y. Tokura, Nature **426**, 55 (2003).
⁸ N. Hur, S. Park, P. A. Sharma, J. S. Ahn, S. Guha, S.W. Cheong, Nature **429**, 392 (2004).
⁹ L.C. Chapon, G. R. Blake, M. J. Gutmann, S. Park, N. Hur, P. G. Radaelli, and S.-W. Cheong, Phys. Rev. Lett. **93**, 177402 (2004).
¹⁰ T. Goto, T. Kimura, G. Lawes, A. P. Ramirez, and Y. Tokura, Phys. Rev. Lett. **92**, 257201 (2004).
¹¹ M. Kenzelmann, A. B. Harris, S. Jonas, C. Broholm, J. Schefer, S. B. Kim, C. L. Zhang, S.-W. Cheong, O. P. Vajk, and J. W. Lynn, Phys. Rev. Lett. **95**, 087206 (2005).
¹² A. Pimenov, A. A. Mukhin, V. Yu. Ivanov, V. D. Travkin, A. M. Balbashov, A. Loidl, Nature Phys. **2**, 97 (2006).
¹³ D. Senff, P. Link, K. Hradil, A. Hiess, L. P. Regnault, Y. Sidis, N. Aliouane, D. N. Argyriou, and M. Braden, Phys. Rev. Lett. **98**, 137206 (2007).
¹⁴ Y. Yamasaki, H. Sagayama, T. Goto, M. Matsuura, K. Hirota, T. Arima, and Y. Tokura, Phys. Rev. Lett. **98**, 147204 (2007).
¹⁵ Y. Yamasaki, S. Miyasaka, Y. Kaneko, J.-P. He, T. Arima, and Y. Tokura, Phys. Rev. Lett. **96**, 207204 (2006).
¹⁶ H. Katsura, N. Nagaosa, and A. V. Balatsky, Phys. Rev. Lett. **95**, 057205 (2005).
¹⁷ I. A. Sergienko and E. Dagotto, Phys. Rev. B **73**, 094434 (2006).
¹⁸ H. Katsura, A. V. Balatsky, and N. Nagaosa, Phys. Rev. Lett. **98**, 027203 (2007).
¹⁹ D. Belitz, T. R. Kirkpatrick, and A. Rosch, Phys. Rev. B **73**, 054431 (2006).
²⁰ B. R. Cooper, in *Solid State Physics*, edited by F. Seitz *et al.* (Academic Press, NY, 1968), Vol. 21, p.293.
²¹ Y. Ishikawa, K. Tajima, D. Bloch, M. Roth, Solid State Commun. **19**, 525 (1976).
²² C. Pfeleiderer, G. J. McMullan, S. R. Julian, and G. G. Lonzarich,

- Phys. Rev. B **55**, 8330 (1997).
- ²³ L. Lundgren, O. Beckman, V. Attia, S. P. Bhattacharjee, and M. Richardson, Phys. Scr. **1**, 69 (1970).
- ²⁴ S. A. Brazovskii and S. G. Dmitriev, JETP **42**, 497 (1976).
- ²⁵ D. R. Nelson and J. Toner, Phys. Rev. B **24**, 363 (1981).
- ²⁶ J. Toner, Phys. Rev. A **27**, 1157 (1983).
- ²⁷ G. Grinstein, T. C. Lubensky, and J. Toner, Phys. Rev. B **33**, 3306 (1986).
- ²⁸ B. I. Halperin and D. R. Nelson, Phys. Rev. Lett. **41**, 121 (1978).
- ²⁹ O. Biham, D. Mukamel, J. Toner, and X. Zhu, Phys. Rev. Lett. **59**, 2439 (1987).